communications earth & environment

Article

https://doi.org/10.1038/s43247-024-01393-9

Shifting sediment depocenters track ice-margin retreat in Baffin Bay

Emmanuel Okuma [1] ✉, Jürgen Titschack [1,2], Jens Weiser [1], Alexandre Normandeau [3], Markus Kienast [4] & Dierk Hebbeln [1]

Reconstructing the depositional history of Baffin Bay allows insights into the deglacial retreat of the Laurentide, Innuitian, and Greenland ice sheets from their maximum extent during the Last Glacial Maximum. Here, we present radiocarbon-controlled sedimentation rates from Baffin Bay based on 79 sediment cores to assess spatio-temporal variabilities in sediment deposition since the Last Glacial Maximum. This comprehensive dataset reveals that until ~15,000 years ago the deep basin and slopes were the dominant active sediment depocenters along most margins of Baffin Bay, suggesting prolonged ice-margin stability near the shelf edge, much longer than previously suggested. Between 13,000-11,000 years ago, most depocenters shifted quickly from the slope to the inner shelf, evidencing a very rapid landward ice-sheet retreat. The sedimentation rate-based mean erosion rates (0.17 and 0.08 millimeters/year) derived from the West Greenland Shelf underscore the high erosion capacity of the western Greenland Ice Sheet draining into Baffin Bay.

Baffin Bay, located between Canada and Greenland, was flanked by three large continental ice sheets during the Last Glacial Maximum (LGM; here considered lasting from ~25 to 18 ka BP)[1–4]. The Laurentide (LIS), Innuitian (IIS), and Greenland (GIS) ice sheets advanced across the continental shelves surrounding Baffin Bay and are postulated to have reached the shelf edge in many places (Fig. 1)[3–7]. In northern Baffin Bay, the LIS and GIS merged with the IIS, forming a continuous ice sheet with an ice shelf[8]. With the deglacial climate warming, the ice sheets retreated landward from their glacial marine-terminating ice margins to their present-day close-to-minimum extent, mainly being confined to onshore settings[9,10]. Around Baffin Bay today, the GIS margin is mostly land-based, while the LIS and IIS have disintegrated into smaller ice masses (e.g., Agassiz, Barnes, and Penny ice caps) and glaciers over Baffin Island and Canadian Arctic Archipelago (Fig. 1c).

Ice-sheet dynamics and the associated changes in the rate and pattern of erosion, and also the mode of sediment transport, had a strong control on sediment deposition in Baffin Bay since the last glacial period[11,12]. However, the reconstruction of the LGM to modern sedimentation history in Baffin Bay is limited by the scarcity of directly dated sediment cores due to the paucity of datable material in the sediments[11–16]. Because recent developments in accelerator mass spectrometry (AMS) dating techniques have reduced the amount of material needed for radiocarbon-based age determinations[17], data availability is increasing rapidly[18–20]. This has led to an increase in field studies providing local information on sedimentation rates in Baffin Bay, including refinements of deglacial ice-margin dynamics (timing/pattern) across the basin[19–23]. Previous reconstructions of paleo-ice sheet extent in Baffin Bay were based largely on undated glacial geomorphological evidence[3,7,9,10]. Despite this progress, no single study to date focuses on the overall development of sedimentation patterns in Baffin Bay since the maximum ice extent during the LGM.

Taking advantage of this data availability, our study presents a new spatio-temporal analysis of radiocarbon-based sedimentation rate patterns across Baffin Bay since the LGM, based on an extensive collection of both previously published ($n = 68$) and new radiocarbon-dated sediment cores ($n = 11$). Besides documenting the successive activation of various depocenters, it provides detailed information on the pattern of ice margin retreat and new sedimentation rate-based estimates of subglacial erosion rates (for the GIS).

Sedimentation in Baffin Bay over the last 25,000 years

Baffin Bay is a >2000 m deep semi-enclosed oceanic basin between the Canadian Arctic Archipelago and Greenland, connecting the Arctic Ocean to the North Atlantic Ocean (Fig. 1). Its continental shelves (up to 500 m deep) are dissected by U-shaped over-deepened cross-shelf troughs (up to 100 km wide and 950 m deep, Fig. 1), that were carved and filled by fast-flowing ice streams associated with the repeated advance of the LIS, IIS, and

[1]MARUM - Center for Marine Environmental Sciences and Faculty of Geosciences, University of Bremen, Bremen, Germany. [2]Senckenberg am Meer, Marine Research Department, Wilhelmshaven, Germany. [3]Geological Survey of Canada (Atlantic), Natural Resources Canada, Dartmouth, NS, Canada. [4]Department of Oceanography, Dalhousie University, Halifax, Canada. ✉e-mail: eokuma@marum.de

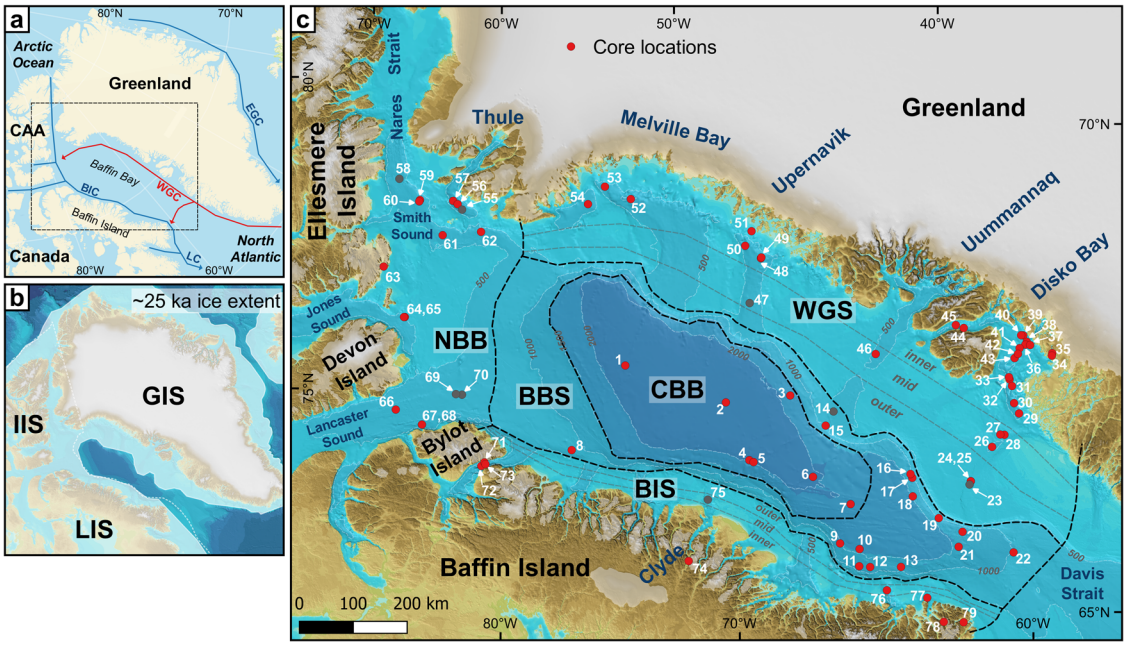

Fig. 1 | Overview maps showing the geographic location of Baffin Bay, its main oceanographic currents and glacial history, and core locations. a Baffin Bay is bordered to the north by the Canadian Arctic Archipelago (CAA), Baffin Island to the west, and Greenland to the east. The Baffin Island Current (BIC) transports colder and fresher waters originating from the Arctic Ocean southwards through Davis Strait, merging with the Labrador Current (LC) flowing into the North Atlantic Ocean. The West Greenland Current (WGC), an admixture of the Arctic-sourced East Greenland Current (EGC) and Atlantic-sourced Irminger Current, carries warmer and more saline waters into Baffin Bay along the west Greenland coast. **b** Reconstructed maximum extent of the Laurentide (LIS), Innuitian (IIS), and Greenland (GIS) ice sheets during the LGM (~25 ka) after Batchelor et al.[3] (solid line) and Dalton et al.[7] (dotted line, truncated around NW Greenland). **c** The location of the 79 radiocarbon-dated sediment cores (filled circles) compiled in this study (gray circles indicate cores with basal till, and red circles without) distributed into six depocenters (differentiated by black and gray dashed lines): (i) Central Baffin Bay (CBB), (ii) Baffin Bay Slope (BBS), (iii) Outer, (iv) Mid, (v) Inner Baffin Island Shelf (BIS) and West Greenland Shelf (WGS), and (vi) Northern Baffin Bay (NBB). Note that all cores taken from an Outer Shelf depocenter are from the WGS and none from the BIS. The locations of cross-shelf troughs on the WGS (e.g., Melville Bay, Upernavik, Uummannaq, Disko Bay) are indicated. The light gray cover represents the present-day ice margin (after Harrison et al.[70]). Bathymetric information in (**b**) and (**c**) is based on the International Bathymetric Chart of the Arctic Ocean Version 3.0[71].

GIS during previous Quaternary glaciations[4,10,24,25]. During full-glacial conditions, the advance of these paleo-ice streams through the cross-shelf troughs enabled the delivery of large volumes of eroded terrigenous and shelf material beyond the trough mouth, forming huge sediment aprons on the adjacent continental slopes, termed trough mouth fans[5,26–29].

The new compilation of 79 ^{14}C-dated sediment cores from Baffin Bay (Fig. 1c and Supplementary Table 1) comprises primarily previously published data complemented by eleven new cores. Only cores with a minimum of two ^{14}C ages, all based on marine micro- and macro-fossil remains, were included in this compilation (see the "Methods" section and Supplementary Table 2). Sedimentation rate (SR) in the majority (86%) of cores in this compilation is constrained by at least three ^{14}C ages, with an overall range of 2–26 ^{14}C ages per core (see the "Methods" section for a rationale of using 2 ages as a minimum and Supplementary Fig. 1). Regionally, the 79 sediment cores are interpreted to represent six individual depocenters, based on a combination of their geographical location, water depth, and relative distance from the present-day coastline (Fig. 1c and Supplementary Table 1): (1) the deep basin (7 cores), which largely comprises water depths >1500 m, termed as Central Baffin Bay (CBB); (2) the slope (15 cores) occupying the water depth interval of ~1500 m until the shelf break (~500 m), referred here as Baffin Bay Slope (BBS); (3) the Outer Shelf (3 cores), with all three cores from the West Greenland Shelf (WGS); (4) the Mid WGS and Baffin Island Shelf (BIS) (8 cores); (5) the WGS and BIS Inner Shelves (30 cores, incl. 4 fjord sites); and (6) the Northern Baffin Bay (NBB) (16 cores), which is treated here as a separate depocenter due to its location at the confluence of the LIS, IIS, and GIS.

The age-depth relationships for these 79 cores were constructed using the rapid Bayesian approach provided by the open-source software UNDATABLE in MATLAB[30]. All ^{14}C ages were re-calibrated applying the Marine20 calibration curve[31] and region-specific marine reservoir age corrections (Supplementary Table 2). The resulting median SRs from UNDATABLE were then binned into 1 ka time-slices (Supplementary Fig. 2 and Supplementary Table 3) and combined in a boxplot for all cores in each depocenter (Fig. 2). In addition, mean SRs were calculated for each sediment core for the four time-intervals considered here (see below and Fig. 3).

As only 8 of the 79 sediment cores from the shelves penetrated the deglacial sediments and reached underlying tills (marked as gray circles in Fig. 1c; see the "Methods" section and Supplementary Fig. 3), we note that the oldest ages retrieved from the cores only present minimum ages of the onset of sedimentation following ice retreat. Cores that did recover tills beneath dated sediments are of exceptional importance, as they permit temporal constraints of ice retreat and the onset of marine sedimentation at the respective site. This is especially useful for the West Greenland Shelf, where previous reconstructions of the timing and pattern of ice-sheet retreat are based largely on near-shore/terrestrial geochronological controls[3,9,23].

From the LGM to ~15 ka BP, sedimentation is only recorded in cores from the CBB and BBS (Fig. 2 and Supplementary Fig. 2). During the LGM (~25 to ~18 ka BP), the median SRs (note that the median SRs is always based on the 1-kyr bins of the median SRs generated by the UNDATABLE age model) were generally low in the CBB, averaging slightly below 10 cm ka^{-1}. In contrast, the BBS cores show higher rates of ~20 cm ka^{-1} (Fig. 2). While rates mainly remained low in the CBB (~10 cm ka^{-1}) during the early deglaciation (~18 to ~12 ka BP), the BBS sites reveal faster accumulation between 30 and 50 cm ka^{-1} (Fig. 2). The following late deglaciation (~12 to ~6 ka BP) is marked by a sharp decrease in the median SRs to <5 and ~10 cm ka^{-1} in the CBB and BBS sites (Fig. 2), respectively, that remained rather constant through the following postglacial period (<6 ka BP).

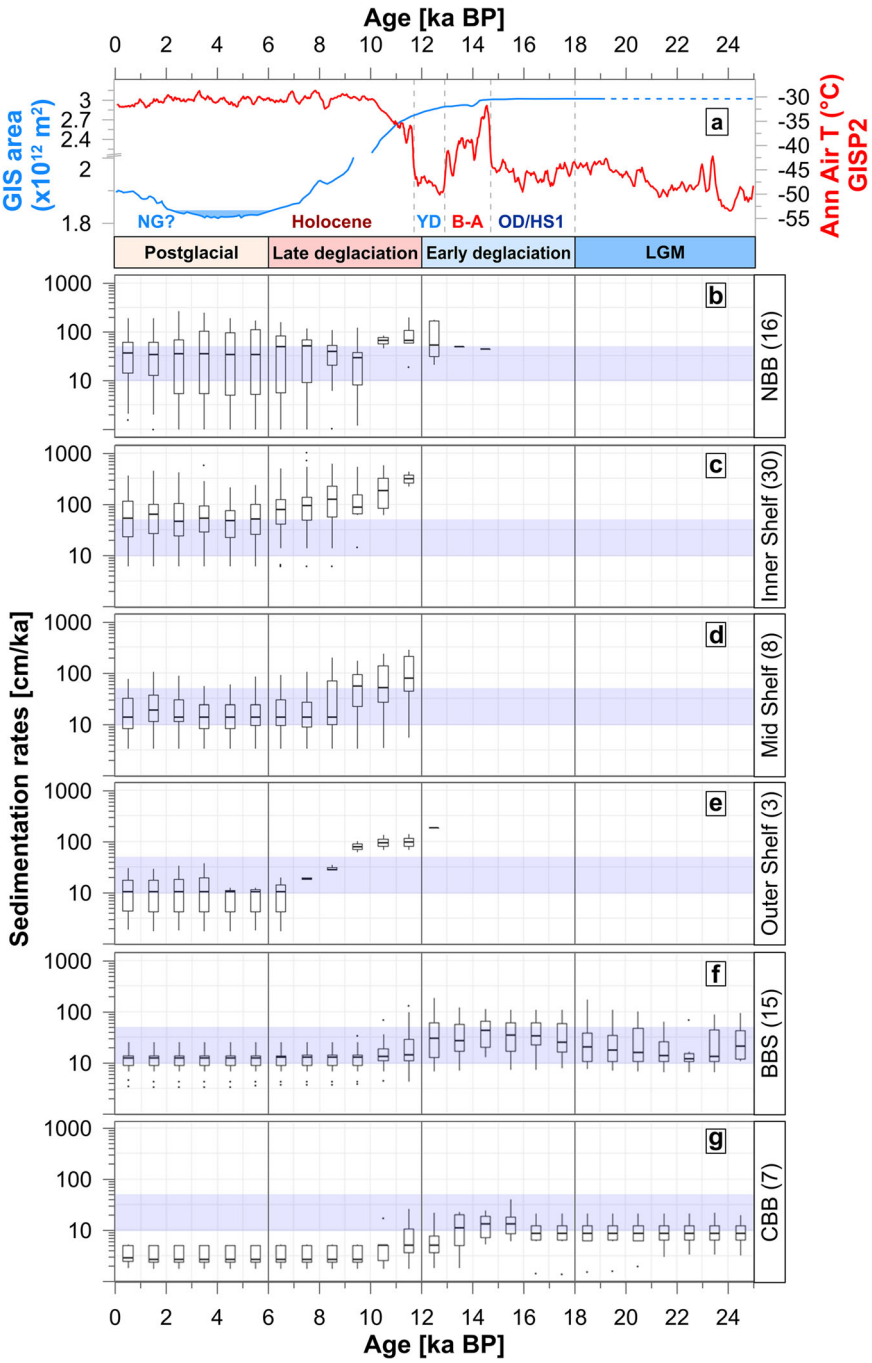

Fig. 2 | Sedimentation rates in Baffin Bay and Greenland Ice Sheet and climate dynamics. 1-kyr-binned sedimentation rates of all sediment cores within a specific depocenter in Baffin Bay are compared with model and proxy reconstructions of Greenland Ice Sheet (GIS) areal extent and air temperature evolution since the Last Glacial Maximum (LGM). **a** The LGM, early deglaciation, late deglaciation, and postglacial intervals are determined based on observed changes in GIS modeled areal extent[37] and reconstructed annual air temperature from proxy data of the GISP2 ice core record[72]. **b–g** Sedimentation rates are separated into the 6 depocenters delineated in Baffin Bay: (i) Central Baffin Bay (CBB), (ii) Baffin Bay Slope (BBS), (iii) Outer Shelf, (iv) Mid Shelf, (v) Inner Shelf, and (vi) Northern Baffin Bay (NBB), with the number of cores in each depocenter is given in brackets. Note that the three shelf depocenters outlined combine cores from the West Greenland Shelf as well as from the Baffin Island Shelf (except for the outer shelf from which no cores exist on the Baffin Island side). The light blue bars mark the sedimentation rate interval of 10–50 cm ka^{-1}. The box plots show the median, minimum, maximum, lower (1st) and upper (3rd) interquartile range, and outliers of sedimentation rates.

The oldest outer shelf record from the WGS has a mean SR of ~200 cm ka^{-1} and dates back to the end (12–13 ka BP) of the early deglaciation (Fig. 2 and Supplementary Fig. 2). During the late deglaciation, median SRs in the outer shelf region drastically declined to ~10 cm ka^{-1} to remain at this level throughout the postglacial. The earliest documented mid- and inner-shelf sedimentation on the BIS and WGS is documented for the late deglaciation (Fig. 2 and Supplementary Fig. 2). On the mid-shelf, median SRs decreased from ~80 cm ka^{-1} to a rather constant ~15 cm ka^{-1} after ~8 ka BP. The inner-shelf median SRs revealed a similar decreasing trend through the late deglaciation, however, on a much higher level, decreasing from ~300 to ~80 cm ka^{-1} (Fig. 2 and Supplementary Fig. 2). Comparably high median SRs of ~50 cm ka^{-1} also persisted throughout the postglacial.

In the NBB, sedimentation is documented since the early deglaciation interval at ~14. 5 ka BP, much earlier than the shelf records from BIS and WGS (Fig. 2 and Supplementary Fig. 2). Median SRs of ~40–70 cm ka^{-1} lasted until about 10 ka BP when during the late deglaciation, the rates decreased to ~30–50 cm ka^{-1}, eventually becoming rather stable around 35 cm ka^{-1} during the postglacial.

Discussion

Spatial sedimentation patterns in Baffin Bay have varied substantially (Figs. 2 and 3) since the LGM, when continental ice (LIS, IIS, GIS) expanded onto the shelves of Baffin Bay (Fig. 1). When the continental ice sheets advanced to or near the shelf breaks during the LGM[3,7,9,10], the CBB and BBS probably were the only accommodation space available as documented by the available sediment cores; therefore, they were most likely the only active depocenters in Baffin Bay (Figs. 2 and 3a). However, sedimentation rates of <20 cm ka^{-1} suggest low terrigenous sediment input into CBB (Figs. 2 and 3). The low amounts of ice-rafted detritus observed in some of

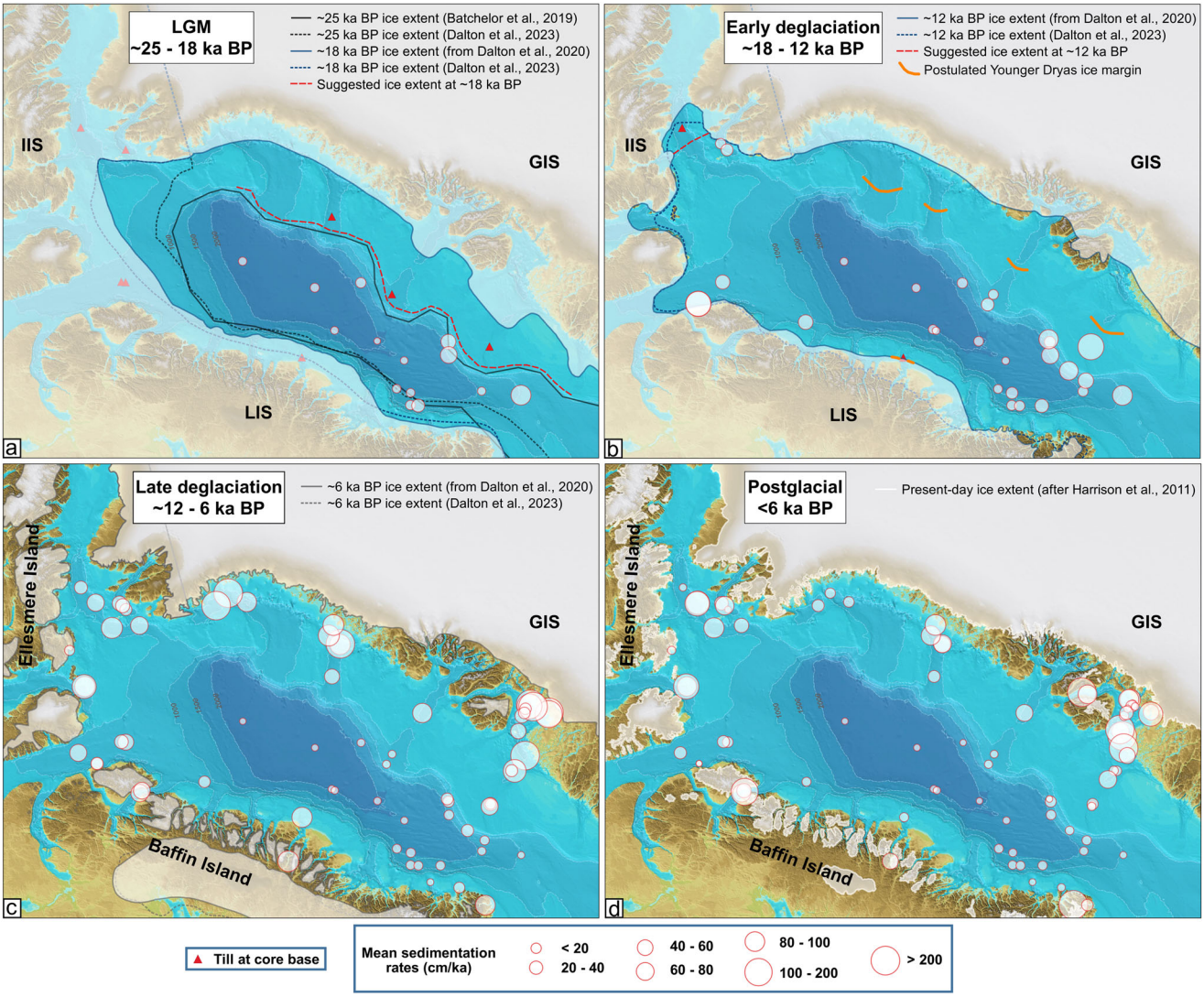

Fig. 3 | Spatio-temporal distribution of sedimentation rates and ice-margin positions in Baffin Bay. The figure depicts the mean sedimentation rates for all individual sediment cores in Baffin Bay across the four-time intervals (**a–d**) considered here and the hypothesized contemporary ice-margin positions. The ~25 ka ice margins (in **a**) are according to Batchelor et al.[3] (solid black line) and Dalton et al.[7] (dotted black line). The ~18 ka BP (in **a**), ~12 ka (in **b**), and ~6 ka BP (in **c**) ice margins are according to Dalton et al.[7] (dotted lines) and from Dalton et al.[10] (solid lines) who adopted the previous Greenland ice-margin reconstruction by Dyke[9]. The red dashed lines highlight new ice margin positions for ~18 (in **a**) and ~12 ka BP (in **b**), respectively, as suggested in this study. The postulated Younger Dryas ice margin (orange lines in **b**) is based on observed grounding zone wedges on the mid-shelf interpreted as periods of ice stillstand or short-term re-advances[20,28,35,43,46,48]. The present-day ice margin (in **d**) is after Harrison et al.[70].

the deep basin records[32,33] point to reduced iceberg rafting and imply sedimentation mainly from turbid meltwater plumes[11,33], which would be consistent with a perennial ice-covered (sea ice and ice-shelf) Baffin Bay during the LGM[8,34]. At the same time, the BBS received more sediment, particularly in the southeastern Baffin Bay off West Greenland (up to 10-fold more, Fig. 3a). There, common glacigenic debris flows and turbidity currents provided the trough mouth fans with high amounts of sediment released from ice streams grounded at the mouths of cross-shelf troughs[5,12], accompanied by sediments delivered by turbid meltwater plumes[34,35].

The higher median SRs in the BBS records observed for the early deglaciation (Fig. 2) indicate faster-accumulating sediments during initial ice sheet recession (Fig. 3). These higher rates reflect the influence of ice-rafted detritus, glacigenic debris flows, and meltwater-induced deposition[34,35]. In contrast, SRs in the more distal CBB only show a slight increase between 13 and 16 ka BP (Fig. 2). During the LGM and the early deglaciation, the fastest deposition occurred at the Disko trough mouth fan in southern Baffin Bay (Fig. 3a, b), suggesting that the feeding glacier, Jakobshavn Isbrae, was most efficient in delivering sediments. This result aligns with present-day observations that indicate that this ice stream is by far the fastest-moving glacier in Greenland[36].

The exclusivity of sedimentation in the CBB and BBS from the LGM to ~15 ka BP (Fig. 2) suggests prolonged ice sheet stability on the Baffin Bay shelves, most likely extending to near the shelf edges, at least within most of the cross-shelf troughs. This observation is consistent with empirical and model reconstructions of the GIS margin denoting close to the full-glacial maximum areal extent during this interval[23,37]. However, local changes in sedimentation style at the slope might indicate an initial small-scale retreat from the very shelf edge off West Greenland, possibly occurring as early as 17 ka BP[34]. Oldest marine sediments overlying a subglacial till were deposited on the upper slope at ~14.8 ka BP[35], followed by outer shelf sedimentation around 13 ka BP[35,38] (Fig. 2). In the NBB, the oldest dated sediments on till have ages of ~14.5 to 15.3 ka BP[19,21], coeval with the collapse of the up to 500 m-thick ice shelf covering northern Baffin Bay[8]. Ice sheet destabilization and the retreat from the shelf edges thus occurred during the relatively warm Bølling–Allerød interstadial[39] and was probably forced by rising northern latitude summer insolation[40,41] and the strengthened

advection of warmer waters into Baffin Bay triggered by the reinvigorated meridional heat transported by the Atlantic Meridional Overturning Circulation (AMOC)[34,42,43]. These data from West Greenland allow us to reassess previously hypothesized ice margin position on the West Greenland shelf at 18 ka BP[9]. The presence of tills and the absence of early-deglaciation sediments on the shelf suggest that at 18 ka BP, the ice still extended to near the edge of the shelf (Fig. 3a).

At the end of the early deglaciation (13–11 ka BP), the main depocenters shifted very quickly from the BBS via the outer shelf to the inner shelf (Fig. 2) (corresponding to 200–300 km on the WGS), indicating an extremely rapid retreat of the ice sheets from the shelf edge towards the coast (see ref. 23). Especially, if also considering that during the Younger Dryas (YD)[44] the ice sheet retreat was halted (or even reversed) as indicated by grounding zone wedges on the Baffin Island and West Greenland shelves[20,28,43,45–48]. During this YD mid-shelf stillstand, SRs were highest at the outer shelf (Figs. 2 and 3b), whereas inner shelf deposition is only documented after the YD cold spell at ~11.5 ka BP (Fig. 2). Although no direct evidence exists, the west Greenland mid-shelf grounding zone wedges and the here proposed later onset of inner-shelf sedimentation suggest that the margin of the GIS persisted on the mid-shelf until 12 ka BP (Fig. 3b, c). Thus, west Greenland inner shelf deglaciation primarily occurred only after the YD cooling in response to early-Holocene climate and ocean warming[49,50].

The fast retreat of the LIS, IIS, and GIS between 13 and 11 ka BP was characterized by massive calving of icebergs leading to enhanced deposition of iceberg-rafted detritus in Baffin Bay, including the widely documented Baffin Bay Detrital Carbonate Layer 0[8,22,51]. Within the cross-shelf troughs, the retreating ice sheets opened new accommodation spaces and, therefore, facilitated shelf deposition that eventually caused sediment starvation in the CBB and BBS depocenters, beginning with the late deglaciation (Fig. 2), resulting in low median SRs for CBB (<5 cm ka^{-1}) and BBS (~10 cm ka^{-1}).

All shelf sections show initially very high SRs that continuously decreased until ~6 ka BP, with the dominant depocenter (i.e., fastest deposition) on the inner shelves (Fig. 2). The high inner shelf SRs are facilitated by the huge accommodation space provided by the overdeepened inner shelf troughs[46], located most proximal to the remaining ice masses. The same pattern of decreasing sedimentation rates during this period is also observed in the NBB (Fig. 2)[19,21]. As a consequence of the shelf deglaciation, sedimentation in Baffin Bay was dominated by hemipelagic sediments over the last 10–8kyr, with only minor contributions from ice-rafted detritus until the beginning of Neoglacial[19,20,45].

During the subsequent postglacial period (<6 ka BP), sedimentation on the shelves leveled off in all areas (Fig. 2). At this time, the LIS and IIS had disintegrated into smaller ice caps over Baffin Island and the Canadian Arctic Archipelago, whereas the GIS attained its Holocene minimum areal extent[10,23,37]. Thus, comparably low median SRs after ~6 ka BP were most likely triggered by reduced sediment input from land to the Baffin Bay shelves, probably due to decreasing sub-ice sheet erosion rates in the postglacial period and from the trapping of meltwater sediment in the inner fjords[52,53]. Still, the highest SRs (>50 cm ka^{-1}) occurred at the most ice-proximal sites on the inner shelves (Figs. 2 and 3d). During the last ~3 ka BP, slightly enhanced median SRs are observed on the inner- and mid-shelves (Fig. 2), probably related to enhanced sediment input caused by Neoglacial re-advance of local glaciers as indicated by renewed ice-rafted detritus sedimentation[19,20,45,54].

Taking advantage of the much better database for the WGS (32 cores; Fig. 1c), we use this comprehensive overview of sedimentation rates to reconstruct erosion rates of the part of GIS draining into the Baffin Bay for the late deglaciation (late deglacial) and postglacial periods. Based on the overall mean of the binned median SR for all cores for these intervals from the four major cross-shelf troughs (Figs. 1c, 3), we calculated mean sediment accumulation rates for each trough (see the "Methods" section). Using the areal extents of the individual troughs and their paleo-ice stream drainages[25], estimated sediment mass fluxes were converted to approximate subglacial erosion rates (Supplementary Table 4; see also refs. 47,48).

Based on the calculated sediment accumulation rates, our estimated late deglacial (12–6 ka BP) bedrock erosion rates for West Greenland range from 0.08 mm yr^{-1} (Uummannaq Trough) to 0.36 mm yr^{-1} (Melville Bay), whereas postglacial rates range from 0.04 to 0.06 mm yr^{-1}, except for Disko Trough with 0.12 mm yr^{-1} (Supplementary Table 4). Although at the lower end, these results largely agree with estimates resulting from geophysical assessments of deglacial sediment volumes in Greenland shelf troughs (0.29–0.52 mm yr^{-1}, these are high estimates due to smaller effective drainage areas considered[55]), from cosmogenic nuclide (^{10}Be) analyses for centennial-scale (0.3–0.8 mm yr^{-1}) and orbital-scale (0.1–0.3 mm yr^{-1}) erosion rates[56,57], and from a 10-year sediment load analysis in a southwest Greenland river (0.5 mm yr^{-1})[58]. The consistency of these estimates based on various methods underlines the high erosion capacity of the GIS, as average subglacial erosion rates of 0.01–0.1 mm yr^{-1} have been given for polar regions[59].

Mean erosion rates derived from all four West Greenland shelf troughs decrease from 0.17 mm yr^{-1} for the late deglacial to 0.08 mm yr^{-1} for the postglacial, reflecting a roughly 55% reduction in subglacial erosion of West Greenland, a trend also observed off Petermann glacier entering Nares Strait[55]. This trend towards decreasing erosion rates probably reflects the transition from active deglacial (ice) retreat to relatively stable postglacial conditions.

Methods

Distribution of ^{14}C ages in cores used in this study

The primary age-control points used in the computation of the SRs for the 79 cores from Baffin Bay, shown in Fig. 2 and Supplementary Fig. 2, range from a minimum of 2 to a maximum of 26 ^{14}C ages per core (Supplementary Fig. 1; our census date is June 30, 2023). Generally, the number and distribution of age-control points in the individual sediment records do have a considerable effect on the information content of the derived SRs, especially on the temporal resolution of the SR record. We decided to use two ages as a lower boundary, as these two ages present the minimum to calculate a reliable SR within the time interval constrained by these two ages, plus an estimate of the SR for the youngest core section assuming a recent age for the core top (see below). Of course, these only give mean values for two sections of the core, potentially masking temporal SR variabilities. Nevertheless, these mean values provide valuable information to assess at least average local SRs. In all the selected depocenters, cores with only a few as well as with a considerable number of ages co-occur (see Supplementary Fig. 1), always revealing a consistent pattern of regional SR development, which even counts for the deep basin cores having the lowest overall numbers of ^{14}C ages (see also Fig. 3). Thus, in sum, higher number of ages per core provide a higher resolved SR record, but even records with only two ages provide valuable information on mean SRs. To limit the related uncertainty, in most cases, we refrain from interpreting SR data from single records but focus on the overall trend in sedimentation patterns, and we advise readers to note this. Despite the limitations mentioned above, these data represent currently our best tool for addressing the glacial to Holocene development of the Baffin Bay sedimentary systems.

Age calibration and sedimentation rates

All ^{14}C ages from each core were re-calibrated individually within the age-depth modeling process of UNDATABLE[30] (settings: nsim = 10^5, bootpc = 30, xfactor = 0.1). For the age calibration, region-specific marine reservoir age correction (ΔR) values[60] were applied to Holocene and deglacial ^{14}C ages (<15,000 years) and a higher ΔR value (250 ± 100 years)[22] for ^{14}C ages > 15,000 years from CBB and BBS (see Supplementary Table 2). As the ^{14}C ages obtained from bulk sediment organic matter and *Portlandia arctica*, due to the "Portlandia Effect," often yield considerably older ages compared to other marine fossils (see refs. 14 and[54–56,61–64]), they were excluded from the age model constructions. In addition, the top of each core is assumed to be of recent age (i.e., 0 ka BP ± 50 years, with recent age defined as the year 1950 AD). We note that the assumption of a modern age of the core top could potentially lead to underestimation of the SR, especially in

cores interpreted to lack younger Holocene sediments[12,21,45,65]. Finally, the topmost (youngest) age for each core was excluded from the bootpc (bootstrapping process) to force the algorithm to include this age in the construction of the age-depth relationship.

Note that the here presented SRs for the Baffin Bay cores were not corrected for any mass-transport deposits as these are usually only documented for those few cores analyzed by computer tomography[18,19] (but see also ref. 12), while for nearby cores with a similar stratigraphy such mass-transport deposits are not documented[21,54,66]. Thus, to treat all records the same way, even the few documented cases[12,19,20] have not been considered. As datings reveal that the sediment in such mass-transport deposits is of rather similar age as in the overlying deposits[18], these mass-transport deposits are also considered to represent time-related sediment input associated with the retreat of ice sheets.

Besides computing the age-depth relationship, UNDATABLE calculates each sediment core's median SRs (in cm ka^{-1}). We binned these rates into one-kiloyear time slices and wrote the mean values to the central position of each slice. The binned SRs are presented in logarithmic scale (log_{10}) in Fig. 2 to emphasize variability in areas (cores) with largely varying values. Additionally, step-plots of the binned SRs for all cores are displayed in Supplementary Fig. 2.

Cores with basal till

Sediment cores that have been interpreted to contain basal till deposits, indicative of paleo-ice extent on Baffin Bay, are indicated (gray-filled circles) in Fig. 1c, including gravity core GeoB22357-3 from the Clyde Trough. The thick diamicton bed (LF2) identified at the bottom of core GeoB22357-3[67] was previously interpreted as a glacigenic debris flows[45]. In light of the newly acquired computed tomographic data (see ref. 19) revealing a rather massive and over-compacted basal diamicton and the absence of any internal structures consistent with glacigenic debris flows (Supplementary Fig. 3; see ref. 67), this basal unit is re-interpreted here as ice-contact sediments. This presence of subglacial till, together with the presented ^{14}C ages, further substantiates evidence that the mid-shelf area of the Clyde shelf trough was glaciated (stillstand or LIS re-advance) by the Clyde Ice Stream during the YD stadial, as postulated by Couette et al.[45].

Estimating subglacial erosion rates

Based on the available late deglacial and postglacial sedimentation rates, assuming an average dry bulk density of 0.8 g cm^{-3} for Greenland fjord and shelf sediments[61] and considering the area covered by the four WGS troughs (Melville, Uummannaq, Upernavik, and Disko)[25], we calculated the total mass accumulation for these four troughs for the two time slices considered here (Supplementary Table 4). As biogenic contributions (total organic carbon and biogenic carbonate) to the sediment accumulation are usually <5%[18,68,69], these have been neglected. In a second step, the calculated mass accumulations were applied to the respective drainage areas[25] to calculate average denudation/erosion rates, thereby considering a density for the predominantly crystalline rocks of 2.7 g cm^{-3} (refs. 47,48). Mean erosion rates for West Greenland have been calculated by averaging the erosion rates of the individual drainage areas of the respective shelf troughs, thereby considering the size of the respective drainage basins.

Of course, there are several limitations to this approach: (1) the limited SR-data coverage for the various troughs on the WGS, as, for example, considering only proximal inner shelf records (e.g., Melville Bay) will lead to an overestimation of the sediment mass accumulation in a trough (and vice versa), (2) the late deglacial rates have to be considered as minimum estimates as most sediment cores considered here did not penetrate the entire deglacial sediment column, thus missing the fast accumulating ice proximal sediments deposited directly after the local deglaciation, and (3) neither sediment bypassing of the troughs, e.g., via iceberg rafting, nor input from the Canadian side is considered. Nevertheless, the consistency of the data from the various investigated cross-shelf troughs, as well as the alignment with estimates based on other methods, underlines the applicability of this approach (see ref. 61).

Data availability

The new ^{14}C ages contributed and data generated in this study are provided in the accompanying Supplementary Information. The computed tomographic data of core GeoB22357-3 is available on the PANGAEA online data repository (https://doi.pangaea.de/10.1594/PANGAEA.965735).

Received: 19 September 2023; Accepted: 15 April 2024;
Published online: 27 April 2024

References

1. Dyke, A. S. et al. The Laurentide and Innuitian ice sheets during the Last Glacial Maximum. *Quat. Sci. Rev.* **21**, 9–31 (2002).
2. Margold, M., Stokes, C. R. & Clark, C. D. Reconciling records of ice streaming and ice margin retreat to produce a palaeogeographic reconstruction of the deglaciation of the Laurentide Ice Sheet. *Quat. Sci. Rev.* **189**, 1–30 (2018).
3. Batchelor, C. L. et al. The configuration of Northern Hemisphere ice sheets through the Quaternary. *Nat. Commun.* **10**, 1–10 (2019).
4. Dalton, A. S., Stokes, C. R. & Batchelor, C. L. Evolution of the Laurentide and Innuitian ice sheets prior to the Last Glacial Maximum (115 ka to 25 ka). *Earth–Sci. Rev.* **224**, 103875 (2022).
5. Li, G., Piper, D. J. W. & Calvin Campbell, D. The Quaternary Lancaster Sound trough-mouth fan, NW Baffin Bay. *J. Quat. Sci.* **26**, 511–522 (2011).
6. Brouard, E. & Lajeunesse, P. Maximum extent and decay of the Laurentide Ice Sheet in Western Baffin Bay during the Last glacial episode. *Sci. Rep*. **7**, 1–7 (2017).
7. Dalton, A. S. et al. Deglaciation of the north American ice sheet complex in calendar years based on a comprehensive database of chronological data: NADI-1. *Quat. Sci. Rev.* **321**, 108345 (2023).
8. Couette, P. O. et al. Evidence for an extensive ice shelf in northern Baffin Bay during the Last Glacial Maximum. *Commun. Earth Environ.* **3**, 1–12 (2022).
9. Dyke, A. S. An outline of North American deglaciation with emphasis on central and northern Canada. *Dev. Quat. Sci.* **2**, 373–424 (2004).
10. Dalton, A. S. et al. An updated radiocarbon-based ice margin chronology for the last deglaciation of the North American Ice Sheet Complex. *Quat. Sci. Rev.* **234**, 106223 (2020).
11. Aksu, A. E. & Piper, D. J. W. Late Quaternary sedimentation in Baffin Bay. *Can. J. Earth Sci.* **24**, 1833–1846 (1987).
12. Jenner, K. A., Campbell, D. C. & Piper, D. J. W. Along-slope variations in sediment lithofacies and depositional processes since the Last Glacial Maximum on the northeast Baffin margin, Canada. *Mar. Geol.* **405**, 92–107 (2018).
13. Aksu, A. E. Baffin Bay in the past 100,000 yr. *Geology* **7**, 245–248 (1979).
14. Aksu, A. E. Holocene and Pleistocene dissolution cycles in deep-sea cores of Baffin Bay and Davis Strait: palaeoceano-graphic implications. *Mar. Geol.* **53**, 331–348 (1983).
15. Andrews, J. T., Jull, A. J. T., Donahue, D. J., Short, S. K. & Osterman, L. E. Sedimentation rates in Baffin Island fiord cores from comparative radiocarbon dates (Canada). *Can. J. Earth Sci.* **22**, 1827–1834 (1985).
16. Andrews, J. T. Late Quaternary marine sediment accumulation in fiord-shelf-deep-sea transects, Baffin Island to Baffin Bay. *Quat. Sci. Rev.* **6**, 231–243 (1987).
17. Mollenhauer, G., Grotheer, H., Gentz, T., Bonk, E. & Hefter, J. Standard operation procedures and performance of the MICADAS radiocarbon laboratory at Alfred Wegener Institute (AWI), Germany. *Nucl. Instrum. Methods Phys. Res. Sect. B* **496**, 45–51 (2021).

18. Saini, J. et al. Holocene variability in sea-ice conditions in the eastern Baffin Bay-Labrador Sea—a north–south biomarker transect study. *Boreas* **51**, 553–572 (2022).
19. Okuma, E. et al. Deglacial and Holocene sediment dynamics and provenances off Lancaster Sound: Implications for paleoenvironmental conditions in northern Baffin Bay. *Quat. Sci. Rev.* **309**, 108101 (2023).
20. Weiser, J., Titschack, J. & Hebbeln, D. The deglaciation of Upernavik trough, West Greenland, and its Holocene sediment infill: processes and provenance. *Boreas* https://doi.org/10.1111/bor.12626 (2023).
21. Kelleher, R. et al. Late glacial retreat of the Lancaster Sound Ice Stream and early Holocene onset of Arctic/Atlantic throughflow in the Arctic Island channels. In *Arctic, Antarctic, and Alpine Research*, Vol. 54, 394–427, (Taylor & Francis, 2022).
22. Jackson, R., Frederichs, T., Schulz, H. & Kucera, M. Chronology of detrital carbonate events in Baffin Bay reveals different timing but similar average recurrence time of North American-Arctic and Laurentide ice sheet collapse events during MIS 3. *Earth Planet. Sci. Lett.* **613**, 118191 (2023).
23. Leger, T. P. M. et al. A Greenland-wide empirical reconstruction of paleo ice-sheet retreat informed by ice extent markers: PaleoGrIS version 1.0. *Clim. Past*. **20**, 701–755, (2024).
24. Praeg, D., Maclean, B. & Sonnichsen, G. Quaternary geology of the Northeast Baffin Island Continental Shelf, Cape Aston to Buchan Gulf (70° to 72°N). Geological Survey of Canada, *Open File* 5409, 1–98 (2007).
25. Batchelor, C. L. & Dowdeswell, J. A. The physiography of High Arctic cross-shelf troughs. *Quat. Sci. Rev.* **92**, 68–96 (2014).
26. Weidick, A. & Bennike, O. Quaternary glaciation history and glaciology of Jakobshavn Isbræ and the Disko Bugt region, West Greenland: a review. *Geol. Survey Denmark & Greenland. Bull.* **14**, 78 (2007).
27. Ó Cofaigh, C. et al. Glacimarine lithofacies, provenance and depositional processes on a West Greenland trough-mouth fan. *J. Quat. Sci.* **28**, 13–26 (2013).
28. Dowdeswell, J. A. et al. Late Quaternary ice flow in a West Greenland fjord and cross-shelf trough system: submarine landforms from Rink Isbrae to Uummannaq shelf and slope. *Quat. Sci. Rev.* **92**, 292–309 (2014).
29. Hofmann, J. C., Knutz, P. C., Nielsen, T. & Kuijpers, A. Seismic architecture and evolution of the Disko Bay trough-mouth fan, central West Greenland margin. *Quat. Sci. Rev.* **147**, 69–90 (2016).
30. Lougheed, B. C. & Obrochta, S. P. A rapid, deterministic age-depth modeling routine for geological sequences with inherent depth uncertainty. *Paleoceanogr. Paleoclimatol.* **34**, 122–133 (2019).
31. Heaton, T. J. et al. Marine20—the marine radiocarbon age calibration curve (0–55,000 cal BP). *Radiocarbon* **62**, 779–820 (2020).
32. Simon, Q., Hillaire-Marcel, C., St-Onge, G. & Andrews, J. T. North-eastern Laurentide, western Greenland and southern Innuitian ice stream dynamics during the last glacial cycle. *J. Quat. Sci.* **29**, 14–26 (2014).
33. Ownsworth, E. et al. Tracking sediment delivery to central Baffin Bay during the past 40 kyrs: Insights from a multiproxy approach and new age model. *Quat. Sci. Rev*. **308**, 1–16 (2023).
34. Jennings, A. E. et al. Ocean forcing of Ice Sheet retreat in central west Greenland from LGM to the early Holocene. *Earth Planet. Sci. Lett.* **472**, 1–13 (2017).
35. Ó Cofaigh, C. et al. An extensive and dynamic ice sheet on the west Greenland shelf during the last glacial cycle. *Geology* **41**, 219–222 (2013).
36. Lemos, A. et al. Ice velocity of Jakobshavn Isbræ, Petermann Glacier, Nioghalvfjerdsfjorden, and Zachariæ Isstrøm, 2015–2017, from Sentinel 1-a/b SAR imagery. *Cryosphere* **12**, 2087–2097 (2018).
37. Lecavalier, B. S. et al. A model of Greenland ice sheet deglaciation constrained by observations of relative sea level and ice extent. *Quat. Sci. Rev.* **102**, 54–84 (2014).
38. Jennings, A. E. et al. Paleoenvironments during Younger Dryas–Early Holocene retreat of the Greenland Ice Sheet from outer Disko Trough, central west Greenland. *J. Quat. Sci.* **29**, 27–40 (2014).
39. Naughton, F. et al. The Bølling–Allerød interstadial. In *European Glacial Landscapes, © 2023 Elsevier Inc., Last Deglaciation,* 45–50, https://doi.org/10.1016/B978-0-323-91899-2.00015-2 (2023).
40. Berger, A. & Loutre, M. F. Insolation values for the climate of the last 10 million years. *Quat. Sci. Rev.* **10**, 297–317 (1991).
41. Laskar, J. et al. A long-term numerical solution for the insolation quantities of the Earth. *Astron. Astrophys.* **428**, 261–285 (2004).
42. Ritz, S. P., Stocker, T. F., Grimalt, J. O., Menviel, L. & Timmermann, A. Estimated strength of the Atlantic overturning circulation during the last deglaciation. *Nat. Geosci.* **6**, 208–212 (2013).
43. Sheldon, C. et al. Ice stream retreat following the LGM and onset of the west Greenland current in Uummannaq Trough, west Greenland. *Quat. Sci. Rev.* **147**, 27–46 (2016).
44. Rasmussen, S. O. et al. A stratigraphic framework for abrupt climatic changes during the Last Glacial period based on three synchronized Greenland ice-core records: refining and extending the INTIMATE event stratigraphy. *Quat. Sci. Rev.* **106**, 14–28 (2014).
45. Couette, P. O. et al. Retreat and stabilization of a marine-based ice margin along a high Arctic Fjord-cross-shelf trough system. *Quat. Sci. Rev.* **302**, 107949 (2023).
46. Slabon, P. et al. Greenland ice sheet retreat history in the northeast Baffin Bay based on high-resolution bathymetry. *Quat. Sci. Rev.* **154**, 182–198 (2016).
47. Newton, A. M. W. et al. Ice stream reorganization and glacial retreat on the northwest Greenland shelf. *Geophys. Res. Lett.* **44**, 7826–7835 (2017).
48. Hogan, K. A. et al. Deglaciation of a major palaeo-ice stream in Disko Trough, West Greenland. *Quat. Sci. Rev.* **147**, 5–26 (2016).
49. Kaufman, D. S. et al. Holocene thermal maximum in the western Arctic (0–180°W). *Quat. Sci. Rev.* **23**, 529–560 (2004).
50. Briner, J. P. et al. Holocene climate change in Arctic Canada and Greenland. *Quat. Sci. Rev.* **147**, 340–364 (2016).
51. Jackson, R. et al. Asynchronous instability of the North American-Arctic and Greenland ice sheets during the last deglaciation. *Quat. Sci. Rev.* **164**, 140–153 (2017).
52. Normandeau, A. et al. Retreat pattern of glaciers controls the occurrence of turbidity currents on high-latitude Fjord Deltas (Eastern Baffin Island). *J. Geophys. Res. Earth Surf*. 0–2 https://doi.org/10.1029/2018JF004970 (2019).
53. Syvitski, J. & Normandeau, A. Sediment redistribution processes in Baffin Island fjords. *Mar. Geol.* **458**, 107024 (2023).
54. Caron, M., Montero-Serrano, J., St-Onge, G. & Rochon, A. Quantifying provenance and transport pathways of Holocene sediments from the northwestern Greenland margin. *Paleoceanogr. Paleoclimatol.* https://doi.org/10.1029/2019pa003809 (2020).
55. Hogan, K. A. et al. Glacial sedimentation, fluxes and erosion rates associated with ice retreat in Petermann Fjord and Nares Strait, north-west Greenland. *Cryosphere* **14**, 261–286 (2020).
56. Young, N. E., Briner, J. P., Maurer, J. & Schaefer, J. M. 10Be measurements in bedrock constrain erosion beneath the Greenland Ice Sheet margin. *Geophys. Res. Lett.* **43**, 11,708–11,719 (2016).
57. Balter-Kennedy, A., Young, N. E., Briner, J. P., Graham, B. L. & Schaefer, J. M. Centennial- and orbital-scale erosion beneath the Greenland ice sheet near Jakobshavn Isbræ. *J. Geophys. Res. Earth Surf.* **126**, 1–27 (2021).
58. Hasholt, B., van As, D., Mikkelsen, A. B., Mernild, S. H. & Yde, J. C. Observed sediment and solute transport from the Kangerlussuaq sector of the Greenland Ice Sheet (2006–2016). *Arctic Antarct. Alp. Res*. **50**, 1–13 (2018).
59. Koppes, M. N. & Montgomery, D. R. The relative efficacy of fluvial and glacial erosion over modern to orogenic timescales. *Nat. Geosci.* **2**, 644–647 (2009).

60. Pieńkowski, A. J., Coulthard, R. D. & Furze, M. F. A. Revised marine reservoir offset (Δ*R*) values for molluscs and marine mammals from Arctic North America. *Boreas* https://doi.org/10.1111/bor.12606 (2022).
61. Andrews, J. T., Milliman, J. D., Jennings, A. E., Rynes, N. & Dwyer, J. Sediment thicknesses and Holocene glacial marine sedimentation rates in three east Greenland Fjords (ca. 68° N). *J. Geol.* **102**, 669–683 (1994).
62. Coulthard, R. D. The complexity of marine 14C chronologies in Arctic Canada: variable Δ*R* values, enhanced deep water reservoirs, and the Portlandia effect. *Quat. Int.* **279–280**, 99 (2012).
63. England, J., Dyke, A. S., Coulthard, R. D., Mcneely, R. & Aitken, A. The exaggerated radiocarbon age of deposit-feeding molluscs in calcareous environments. *Boreas* **42**, 362–373 (2013).
64. Jackson, R. et al. Holocene polynya dynamics and their interaction with oceanic heat transport in northernmost Baffin Bay. *Sci. Rep*. **11**, 1–17 (2021).
65. Furze, M. F. A., Pieńkowski, A. J., McNeely, M. A., Bennett, R. & Cage, A. G. Deglaciation and ice shelf development at the northeast margin of the Laurentide Ice Sheet during the Younger Dryas chronozone. *Boreas* **47**, 271–296 (2018).
66. Giraudeau, J. et al. A high-resolution elemental record of post-glacial lithic sedimentation in Upernavik Trough, western Greenland: history of ice-sheet dynamics and ocean circulation changes over the last 9100 years. *Glob. Planet. Change* **191**, 103217 (2020).
67. Okuma, E., Titschack, J. & Hebbeln, D. *Processed CT Image of Sediment Core GeoB22357-3 from Western Baffin Bay, Maria S. Merian cruise MSM66* https://doi.pangaea.de/10.1594/PANGAEA.965735 (2024).
68. Perner, K., Moros, M., Jennings, A., Lloyd, J. M. & Knudsen, K. L. Holocene palaeoceanographic evolution off West Greenland. *Holocene* **23**, 374–387 (2013).
69. Limoges, A. et al. Learning from the past: Impact of the Arctic Oscillation on sea ice and marine productivity off northwest Greenland over the last 9,000 years. *Glob. Chang. Biol.* **26**, 6767–6786 (2020).
70. Harrison, J. C. et al. *Geological Map of the Arctic; Geological Survey of Canada, Map 2159A, scale 1/5 000 000*. 1–5 (Geological Survey of Canada, 2011).
71. Jakobsson, M. et al. The International bathymetric chart of the Arctic Ocean (IBCAO) version 3.0. *Geophys. Res. Lett*. https://doi.org/10.1029/2012GL052219 (2012).
72. Alley, R. B. The Younger Dryas cold interval as viewed from central Greenland. *Quat. Sci. Rev.* **19**, 213–226 (2000).

Acknowledgements

We thank the masters and crew members of the various cruises who recovered the Baffin Bay sediment cores used in this study and those involved in the work to obtain radiocarbon ages. Sample materials have been provided by the GeoB Core Repository at the MARUM—Center for Marine Environmental Sciences, University of Bremen, Germany. We are grateful to the respective authorities of Canada, Denmark, Greenland, and Nunavut for granting the permits to collect sediment cores during RV CCGS Hudson expedition 2018042 and RV Maria S. Merian expeditions MSM44 and MSM66 from the 11 new core sites introduced by this study. We also thank Dr. Martin Bartels for sample preparation for radiocarbon dating and Dr. Lucas Jonkers and Dr. Michael Siccha for their support during the data analysis phase of this manuscript. This project was supported by the Deutsche Forschungsgemeinschaft (Bonn, Germany) through the International Research Training Group "Processes and impacts of climate change in the North Atlantic Ocean and the Canadian Arctic" (IRTG 1904 ArcTrain). We also appreciate the insightful comments from Martin Margold and two anonymous reviewers that greatly improved this manuscript.

Author contributions

E.O., J.T., M.K., and D.H. conceived this research work.; E.O. compiled and acquired data with additional data from J.W. and A.N.; E.O. conducted literature reviews with input from J.T. and D.H.; E.O. analyzed the data and wrote the first manuscript draft, and all other authors contributed to improving this draft; E.O. prepared figures and supplementary information and wrote the methods with input from all other authors; E.O. revised the manuscript with contributions from all other authors; J.T., M.K., and D.H. supervised this research.

Funding

Open Access funding enabled and organized by Projekt DEAL.

Competing interests

The authors declare no competing interests.

Additional information

Supplementary information The online version contains supplementary material available at https://doi.org/10.1038/s43247-024-01393-9.

Correspondence and requests for materials should be addressed to Emmanuel Okuma.

Peer review information *Communications Earth & Environment* thanks Marit-Solveig Seidenkrantz, Martin Margold, and Timothy Lane for their contribution to the peer review of this work. Primary Handling Editors: Ola Kwiecien, Alireza Bahadori and Aliénor Lavergne. A peer review file is available.